4 channel × 10 Gb/s bidirectional optical subassembly using silicon optical bench with precise passive optical alignment

Eun Kyu Kang,[1] Yong Woo Lee,[1] Sooraj Ravindran,[2] Jun Ki Lee,[3] Hee Ju Choi,[4] Gun Wu Ju,[1] Jung Wook Min,[4] Young Min Song,[5] Ik-Bu Sohn,[3] and Yong Tak Lee[1,*]

[1]*School of Information and Communications, Gwangju Institute of Science and Technology, Gwangju 500-712, South Korea*
[2] *Department of Avionics, Indian Institute of Space science and Technology, Valiamala, Trivandrum, 695-547, India*
[3]*Advanced Photonics Research Institute, Gwangju Institute of Science and Technology, Gwangju 500-712, South Korea*
[4]*Department of Physics and Photon Science, Gwangju Institute of Science and Technology, Gwangju 500-712, South Korea*
[5]*Department of Electronic Engineering, Pusan National University, Busan, 609-735, South Korea*
[*]*ytlee@gist.ac.kr*

Abstract: We demonstrate an advanced structure for optical interconnect consisting of 4 channel × 10 Gb/s bidirectional optical subassembly (BOSA) formed using silicon optical bench (SiOB) with tapered fiber guiding holes (TFGHs) for precise and passive optical alignment of vertical-cavity surface-emitting laser (VCSEL)-to-multi mode fiber (MMF) and MMF-to-photodiode (PD). The co-planar waveguide (CPW) transmission line (Tline) was formed on the backside of silicon substrate to reduce the insertion loss of electrical data signal. The 4 channel VCSEL and PD array are attached at the end of CPW Tline using a flip-chip bonder and solder pad. The 12-channel ribbon fiber is simply inserted into the TFGHs of SiOB and is passively aligned to the VCSEL and PD in which no additional coupling optics are required. The fabricated BOSA shows high coupling efficiency and good performance with the clearly open eye patterns and a very low bit error rate of less than 10^{-12} order at a data rate of 10 Gb/s with a PRBS pattern of 2^{31}-1.

©2016 Optical Society of America

OCIS codes: (060.2360) Fiber optics links and subsystems; (140.3325) Laser coupling; (200.4650) Optical interconnects; (220.1140) Alignment; (230.0230) Optical devices.

References and links

1. S. H. Hwang, D. D. Seo, J. Y. An, M.-H. Kim, W. C. Choi, S. R. Cho, S. H. Lee, H.-H. Park, H. S. Cho, S. H. Hwang, D. D. Seo, J. Y. An, M.-H. Kim, W. C. Choi, S. R. Cho, S. H. Lee, H.-H. Park, and H. S. Cho, "Parallel optical transmitter module using angled fibers and a V-grooved silicon optical bench for VCSEL array," IEEE Trans. Adv. Packag. **29**(3), 457–462 (2006).
2. F. E. Doany, C. L. Schow, C. W. Baks, D. M. Kuchta, P. Pepeljugoski, L. Schares, R. Budd, F. Libsch, R. Dangel, F. Horst, B. J. Offrein, and J. A. Kash, "160 Gb/s bidirectional polymer-waveguide board-level optical interconnects using CMOS-Based transceivers," IEEE Trans. Adv. Packag. **32**(2), 345–359 (2009).
3. K. Nakama, Y. Matsuzawa, Y. Tokiwa, and O. Mikami, "Board-to-board optical plug-in interconnection using optical waveguide plug and micro hole array," IEEE Photonics Technol. Lett. **23**(24), 1881–1883 (2011).
4. S. H. Hwang, J. Y. An, M.-H. Kim, W. C. Choi, S. R. Cho, S. H. Lee, H. S. Cho, and H.-H. Park, "VCSEL array module using (111) facet mirrors of a V-grooved silicon optical bench and angled fibers," IEEE Photonics Technol. Lett. **17**(2), 477–479 (2005).
5. H.-C. Lan, H.-L. Hsiao, C.-C. Chang, C.-H. Hsu, C.-M. Wang, and M.-L. Wu, "Monolithic integration of diffractive optical element on silicon 45-degree micro-reflector," in *Conference on Optical Fiber Communication - Incudes Post Deadline Papers, 2009* (OFC, 2009), pp. 1–3.
6. P.-K. Shen, C.-T. Chen, C.-C. Chang, H.-L. Hsiao, Y.-C. Chang, S.-L. Li, H.-Y. Tsai, H.-C. Lan, Y.-C. Lee, and M.-L. Wu, "Optical interconnect transmitter based on guided-wave silicon optical bench," Opt. Express **20**(9), 10382–10392 (2012).

7. B. S. Rho, S. Kang, H. S. Cho, H.-H. Park, S.-W. Ha, and B.-H. Rhee, "PCB-compatible optical interconnection using 45 deg;-ended connection rods and via-holed waveguides," J. Lightwave Technol. **22**(9), 2128–2134 (2004).
8. M. Schneider, T. Kühner, J. Mohr, and D. Maas, "Fibers in printed circuit boards with passively aligned coupling," J. Lightwave Technol. **28**(15), 2121–2128 (2010).
9. D. Xinyuan, X. Wang, X. Lin, D. Ding, D. Z. Pan, and R. T. Chen, "Highly flexible polymeric optical waveguide for out-of-plane optical interconnects," Opt. Express **18**(15), 16227–16233 (2010).
10. S.-H. Hsu, C.-Y. Tsou, C.-M. Wang, and S.-C. Tseng, "10 Gb/s optical interconnection on flexible optical waveguide in electronic printed circuit board," Opt. Photonics J. **3**(2), 252–255 (2013).
11. J. Sangirov, G.-C. Joo, J.-S. Choi, D.-H. Kim, B.-S. Yoo, I. A. Ukaegbu, N. T. H. Nga, J.-H. Kim, T.-W. Lee, M. H. Cho, and H.-H. Park, "40 Gb/s optical subassembly module for a multi-channel bidirectional optical link," Opt. Express **22**(2), 1768–1783 (2014).
12. H.-L. Hsiao, H.-C. Lan, C.-C. Chang, C.-Y. Lee, S.-P. Chen, C.-H. Hsu, S.-F. Chang, Y.-S. Lin, F.-M. Kuo, J.-W. Shi, and M.-L. Wu, "Compact and passive-alignment 4-channel x 2.5-Gbps optical interconnect modules based on silicon optical benches with 45 degrees micro-reflectors," Opt. Express **17**(26), 24250–24260 (2009).
13. C.-T. Chen, H.-L. Hsiao, P.-K. Shen, G.-F. Lu, H.-C. Lan, Y.-C. Lee, C.-C. Chang, J.-Y. Li, A. Nedle, S.-F. Chang, Y.-S. Lin, and M.-L. Wu, "Miniaturized bidirectional optical subassembly using silicon optical bench with 45-deg micro-reflectors in short-reach 40-Gbit/s optical interconnects," Opt. Eng. **51**(11), 115005 (2012).

1. Introduction

Recently, optical interconnection systems are gaining attention as the prime candidate which can satisfy the huge demand for high-speed data transmissions and can overcome the limitation of electrical interconnects owing to their several advantages such as wide bandwidth, low signal loss, small volume, low power consumption, and immunity to electromagnetic interference, compared with conventional copper-based electrical interconnects. In order to accelerate the usage of optical interconnections in high-speed data transmissions and data storage center, developing low-cost and low power consumption optical modules that are assembled with a simple process is highly needed [1−3]. In case of short-reach optical interconnection, many advanced technologies, such as silicon optical bench (SiOB) with 45° mirror [4–6], optical printed circuit board (OPCB) [7, 8], polymer waveguides [9, 10], and angled fiber [11] have been introduced in order to meet higher channel density integration and/or easy assembly process so as to achieve lower cost and mass production. However, all of the above mentioned schemes have several drawbacks making them less popular as the scheme for optical interconnects.

For example, SiOB with 45° mirror configuration [12, 13] has a large mirror loss as the 45° mirror does not have 100% reflectivity, leading to loss of optical power. Furthermore, the distance between laser, 45° mirror and fiber as well as between fiber, 45° mirror and photodetector is typically greater than 100 μm. Due to this long optical path length, the maximum coupling efficiency in this scheme is quite low (≤ −5 dB). Other schemes such as OPCB [7] uses multimode polymer waveguides which require a core thickness greater than 20 μm making the fabrication difficulty. Angled fiber scheme [11] also have drawbacks similar to that of 45° mirror configuration. Furthermore, the alignment is not passive (i.e, it requires additional coupling optics), and requires additional fabrication steps such as lapping and polishing for forming 45° angled fiber, which complicates the overall fabrication steps, thereby increasing the cost. It is therefore of paramount importance to design and realize SiOB based optical interconnect scheme that is simpler to fabricate, cost effective and more efficient.

In this paper, we have designed and fabricated a SiOB based bidirectional optical subassembly (BOSA) with multi-channel transmitter (Tx) and receiver (Rx) as the optical engine of optical interconnects to achieve the mass production, easy assembly, and high-level of alignment accuracy of optoelectonic devices-to-multi mode fiber (MMF), which can over come the drawbacks of conventional optical interconnect schemes that are described above. The proposed SiOB based BOSA consist of the 12-channel tapered fiber guiding holes (TFGHs), guide pin holes (GPHs), and high-speed coplanar waveguide transmission line (CPW Tline). The fiber guidng holes allow easy alignment of optoelectronic devices with that of multi-mode fiber without the requirement of additional coupling optics. This passive alignment scheme therefore greatly simplifies the alignment process, thereby ensuring high

coupling efficiency which is very cruitial for attaining good overall performance. Prior to fabrication of the proposed SiOB based BOSA, theoretical calculations were carried out based on ray-tracing method to evaluate the optical coupling efficiency, and a 3D full-wave electromagnetic field simulations were carried out to evaluate the insertion loss of the CPW Tline [10, 12, 13]. The high-speed operated vertical-cavity surface-emitting laser (VCSEL) and the photodiode (PD) array were attached at the end of CPW Tline using a high-precision filp-chip bonder, and as a result, the error due to mis-alignment between optoelectonic devices (VCSEL and PD array) and MMF is greatly minimized. The optoelectronic devices and the MMF are automatically aligned thanks to TFGHs, which can decrease the production time and increase the system reliability.

We find that the fabricated SiOB based BOSA with 4 channel Tx and PD has a very high optical coupling efficiency and a bit error rate (BER) smaller than 10^{-12} based on MMF system, making them highly suitable for short-reach optical interconnect applications.
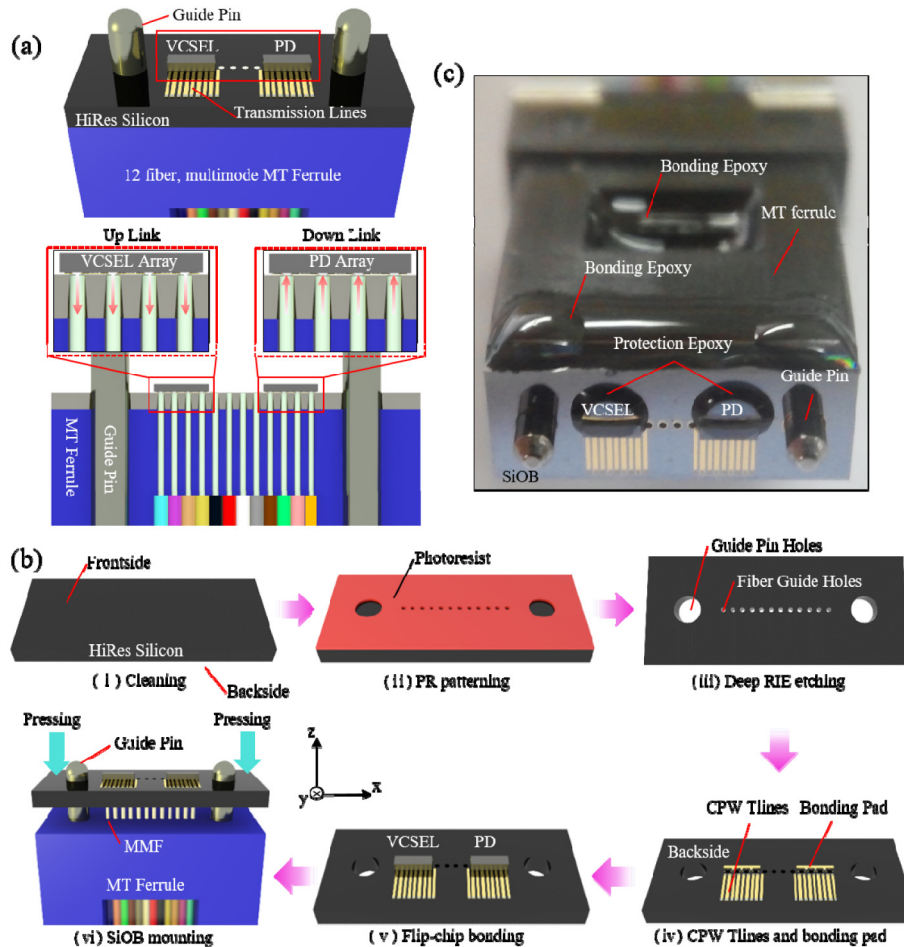

Fig. 1. (a) (Top) Schematic illustration of proposed SiOB-based bidirectional optical subassembly (BOSA). (a) (Bottom) Arrows indicate the optical path of the SiOB-based BOSA. (b) Schematic illustration of the process steps for the fabrication of SiOB-based BOSA. (c) Photograph of the fabricated SiOB-based BOSA.

2. Design of the bidirectional optical subassembly

Figure 1(a) shows the schematic of the proposed SiOB-based BOSA realized using a passive optical aligment process. The BOSA consists of a 4 channel VCSEL array and a 4 channel p-

i-n PD array, a SiOB with TFGHs, a 12 channel MT ferrule with guide pin, and a 12 channel ribbon fiber. In this structure, VCSEL and PD array are fiip-chip bonded onto the high-speed CPW Tline of SiOB. The VCSEL and PD-bonded SiOB is joined to the MT ferrule using a 12 channel ribbon fiber, as shown in Fig. 1(a). In the fabrication of these BOSAs, we used high resistivity silicon substrate having a resistivity over 5000 Ohm-cm, and a standard OM3 MMF whose core and clad diameter is 50 μm and 125 μm, repectively. For active components, we used commercially available high-speed operated VCSEL and p-i-n based PD array made by Ulm Photonics Inc.

Figure 1(a) (Bottom) show the passive optical alignment process which helps in obtaining precise alignment. The 12 channel ribbon fiber whose length is 710 μm from the end face of MT ferrule is inserted through the hole having a larger diameter of Tapered Fiber Guide. The total distance between the optoelectronic devices and MMF is less than 10 μm. This scheme therefore does not require any additional coupling optics which greatly reduces the cost, and further ensures that the emitted light from VCSEL is perfectly coupled with MMF, leading to high coupling efficiency and better performance. The coupled light then passes through the MMF and then reaches the PD, as shown Fig. 1(a) (Bottom).

2.1 Detailed fabrication steps of a BOSA with SiOB and MT ferrule

Figure 1(b) illustrates the various steps involved in the fabrication of the proposed BOSA. First, an 8 inch diameter double side polished high resistivity silicon substrate (HiRes Si) having a thickness of 715 μm was used in this study. A conventional photolithography process was performed on the frontside of HiRes Si to form photoresist (PR) mask patterns for GPHs and TFGHs, as shown in Fig. 1(ii). The diameter of the two patterns for GPHs and TFGHs is 710 μm and 140 μm, respectively. GPHs and TFGHs on the HiRes Si were formed by Bosch deep reactive ion etching (DRIE). The diameter of the hole in the frontside and backside of TFGHs is 140 μm and 125 μm, respectively. Ti/Au (100/500 nm) metal was deposited on the backside of the perforated HiRes Si using e-beam evaporator to form the high-speed CPW Tline. The formed Tline (see Fig. 1(iv)) had signal line of width 85 μm, ground line of width 65 μm, and a gap of 50 μm between them, which had an insertion loss of −0.52 dB at 10 GHz. Then, a 4000 nm thick $Sn_{96.5}Ag_{3.0}Cu_{0.5}$ was deposited at the end of the CPW Tline for filp-chip bonding of VCSEL and PD array. VCSEL and PD array were attached on the SiOB using a high-precision filp-chip bonder, resulting in structure as shown Fig. 1(v). Additionally, the mounted VCSEL and PD arrays were covered with UV curable epoxy to enhance the stability of electrical connection. Finally, the fabricated SiOB was mounted on MT ferrule with ribbon fiber using the GPHs of SiOB and guide pin of MT ferrule, as illustrated in Fig. 1(vi).
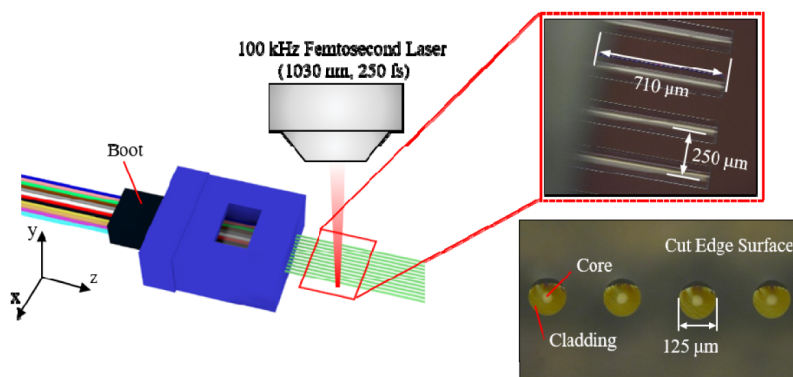

Fig. 2. Schematic diagram of ribbon fiber cleaving using a femtosecond laser for high precision control of fiber length. (right top) Microscope image of a cutted ribbon fiber, and (right bottom) image for cut edge surface.

To prepare the MT ferrule with 710 μm long fiber from the end face of MT ferrule, we used a 100 kHz femtosecond laser for cleaving, as illustrated in Fig. 2. Although the cladding of fiber was slightly damaged by this laser cleaving, the core of the fiber was not affected, as shown inset of Fig. 2.

2.2 Fabrication of perforated holes on HiRes Si

The plane and cross-sectional view of the perforated holes formed on HiRes Si using DRIE process is shown in Fig. 3. In order to obtain the desired diameter for the front and backside holes, we PR pattern having diameters of 125, 130, 135, and 140 μm. The difference in the diameter of the hole in the front and backside holes was approximately 5 μm in all the samples. The plane and vertical etching profile of the hole fabricated using a 140 μm PR pattern is shown in Figs. 3(a) and 3(b). The hole diameter at the front and backside was 140 μm and 125 μm, respectively. The maximum tilt angle of the fiber was <1° ensuring good alignment. Furthermore, the fabricated hole had a tapered etch profile which not only helps in inserting the MMF but also enhances the optical alignment between active optoelectronic devices and MMF. Therefore, we can expect precise optical alignment by using TFGHs.
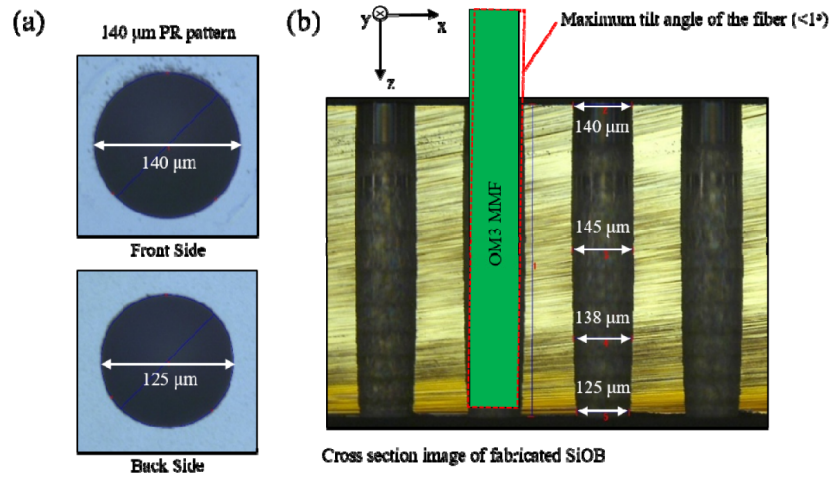

Fig. 3. (a) Front and back side view of silicon substrate with perforated hole for 140 μm PR patterns. (b) Cross sectional image of the fabricated SiOB with tapered hole arrays.
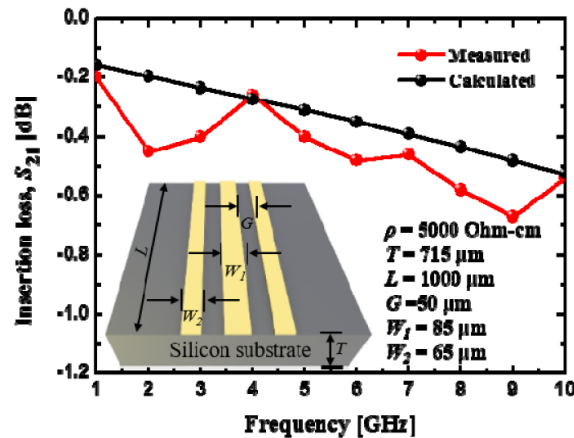

Fig. 4. Calculated and fabricated insertion loss (S_{21}) of the CPW Tline as a function of frequency. Inset indicates the calculation model, where L is the length of CPW Tline, G is the gap, W_1 is the signal line width, W_2 is the ground line width, and T is the substrate thickness.

3. Simulation of electrical and optical properties

3.1 Design and fabrication of CPW Tline

In order to analyze the electrical performance of proposed SiOB, insertion loss S_{21} of the performance of designed standard Au CPW Tline was evaluated using 3D full-wave electromagnetic field software simulator (HFSS) [6], as function of operating frequency. Using HFSS software, designed Au CPW Tline for substrate resisitivities from 10^2 to 10^4 Ohm-cm were simulated, and provided the insertion loss S_{21} of −0.65 dB to −0.50 dB under the fixed parameter. i.e., length (L) as 1000 μm, gap (G) as 50 μm, signal line width (W_1) as 85 μm, ground line width (W_2) as 65 μm, Au trace thickness as 500 nm, and substrate thickness (T) as 715 μm. Figure 4 shows the S_{21} of calculated and fabricated Au CPW Tline on HiRes Si substrate. The fabricated Au CPW Tline showed a low S_{21} of −0.52 dB which results shows a good agreement between the HFSS simulations at 10 Ghz as shown Fig. 4.

3.2 Calcutation of optical coupling efficiency of VCSEL-to-MMF-to-PD

The performance of optical interconnect module is greatly decided by the optical coupling efficiency between the optoelectronic devices and MMF. Therefore, A ray-tracing simulation software (LightTools) is used to evaluate the optical coupling efficiency between VCSEL, PD and MMF of proposed SiOB. Figure 5(a) illustrates the simulation model used in calculating the coupling efficiency. The VCSEL emitting at λ = 850 nm had a beam divergence of 23° and an aperture of 10 μm. The aperture of PD was 55 μm, and the MMF had a core diameter of 50 μm (refractive index n = 1.47) and a cladding diameter of 125 μm (refractive index n = 1.45). The distance between the optoelectronic device and the end face of MMF was set at 10 μm. Fresnel reflection at the surface of the core was not considered in the calculation.
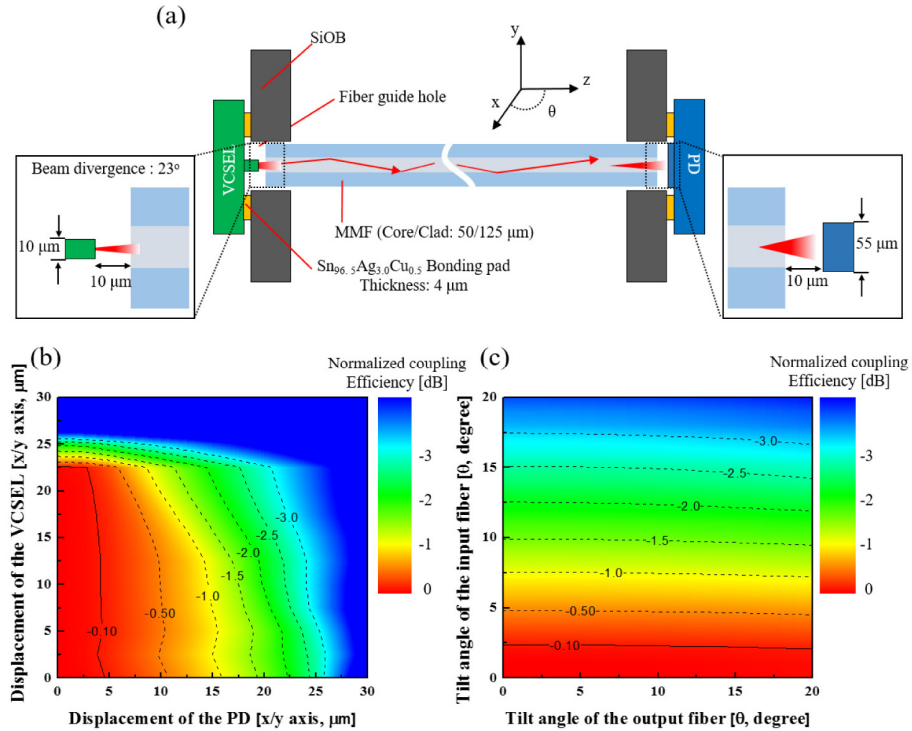

Fig. 5. (a) Schematic illustration of the simulation model for calculating the coupling efficiency of VCSEL-to- MMF (Tx) and MMF-to-PD (Rx). (b-c) Contour plot of calculated normalized coupling efficiency in accordance with (b) displacement of VCSEL and PD and (c) tilt angle of the input and output fiber.

Ray-tracing results show that an in-plane displacement of the PD by 5μm and 15μm results in a coupling penalty of −0.1 dB and −1.0 dB, respectively. While an in-plane displacement of the VCSEL by 22 μm and 24 μm results in a coupling penalty of −0.1 dB and −1.0 dB, respectively, as shown Fig. 5(b). The coupling is very insensitive to the tilt-angle of the output fiber, and has a −1 dB penalty for a 7.5° tilt angle (θ) of the input fiber, as shown Fig. 5(c). It is noteworthy that in our proposed structure, the tilt angle did not exceed 1° as shown in Fig. 3(b). Thus, our proposed structure could ensure that the coupling loss due to angular misalignment is nearly zero.

4. Charaterization of the proposed BOSA

4.1 Measurement of coupling efficiency between VCSEL-to-MMF

Figure 6 shows the schematic illustration of the optical path from the VCSEL-to-MMF as a function of fiber cutting length inside SiOB. As described in Fig. 6, fiber cutting length is closley related to the optical path. Thus, the proposed BOSA was built by using MT ferrules having a fiber cutting length of 710, 680, 650, and 620 μm. Table 1. shows the measurement conditions and the coupling efficiency of the VCSEL-to-MMF (Tx) for various fiber cutting length. The coupled optical power was measured using an optical power meter. The VCSEL array was biased at 6 mA, and all the VCSELs of the channel had similar forward voltage (1.89 ~1.91 V). Therefore, we assumed that the VCSELs used in our study had similar output power. Among the built BOSAs, the BOSA with a fiber cutting length of 710 μm showed the highest coupling efficiency of about −0.008 dB excluding Fresnel reflection loss due to the least x/y and tilt angle misalignment. The coupling efficiency of BOSA made with a fiber cutting length of 650 μm also had a relatively high coupling efficiency of −0.115 dB. This indicates the fiber cutting length can have a tolerance of upto 60 μm so as to obtain high coupling efficiency. The 4-channel Tx having a fiber cutting length of 710 μm shows the similar high coupling efficiency, as summarized in Table 2.
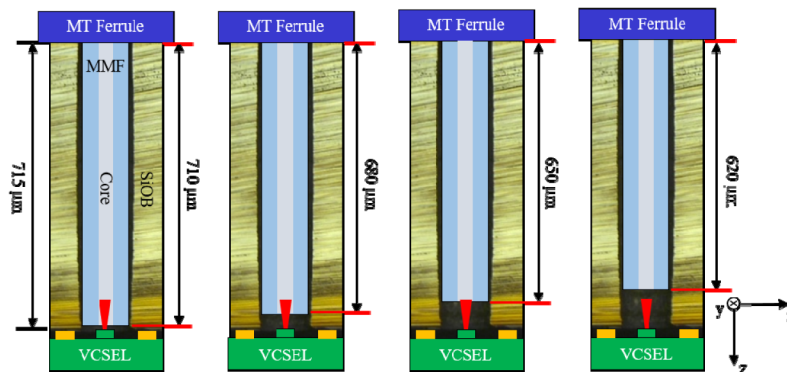

Fig. 6. Schematic illustration of distance from the VCSEL to MMF for four different MMF length.

Table 1. Measured coupling efficiency for four different fiber cutting length.

Fiber Cutting Length [μm]	Reference	710	680	650	620
Output Power [mW]	2.130	2.126	2.120	2.074	1.982
Normalized Coupling Efficiency [dB]	0	−0.008	−0.020	−0.115	−0.440

Table 2. Measured coupling efficiency of 4-channel Tx.

Channel	Reference	Ch1	Ch2	Ch3	Ch4
Output Power [mW]	2.130	2.126	2.127	2.126	2.126
Normalized Coupling Efficiency [dB]	0	−0.008	−0.006	−0.008	−0.008

4.2 Measurement of eye patterns and bit error rate of the fabricated BOSA

To verify the high-speed performance of the fabricated 4 channel × 10 Gb/s BOSA without the VCSEL driver and transimpedance amplifier (TIA) IC, the 4 channel eye diagrams are measured. Figure 7 shows the block diagram of the setup used for measuring the eye patterns without VCSEL driver and TIA. The modulated 10 Gb/s non-return-to-zero signals are generated by a pulse pattern generator and a bias current of 6 mA generated by a sourcemeter are fed into the CPW Tline of transmitting part of SiOB 1 via a bias tee 1 and ground-signal-ground (GSG) RF probe 1. The reverse bias voltage of 2 V generated by power supply is fed into the CPW Tline of receiving part of SiOB 2 via bias tee and GSG RF probe 2. The modulated optical signals are transmitted to the PD array via a 10 m 4-channel MMF. The electrical signals generated by the PD array are detected using a wide-bandwidth oscilloscope. The bottom right image in Fig. 7 (bottom right) shows the measured electrical eye patterns for the 10 Gb/s data with a pseudo random binary sequence (PRBS) pattern of 2^{31}-1. The measured four channels show clear eye opening and have the similar eye-pattern indicating that the fabricated BOSA can be successfully operated at a data rate of 10 Gb/s.
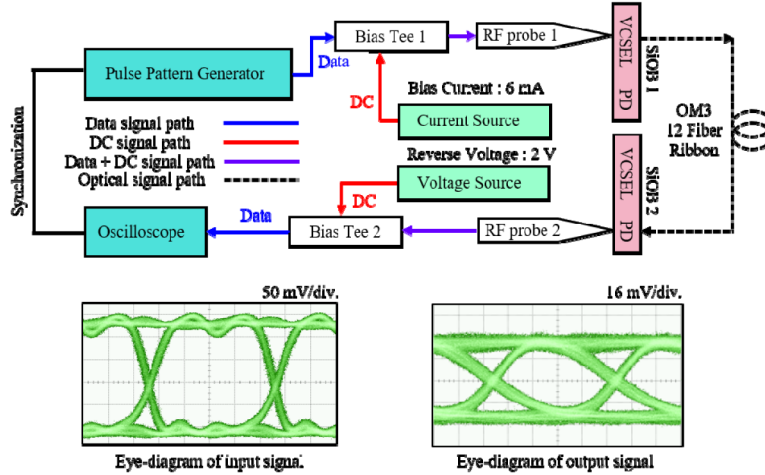

Fig. 7. Experimental setup to measure the eye patterns of the proposed BOSA. Note that the test is carried out without VCSEL driver and TIA. (bottom left) Input PRBS pattern of 2^{31}-1 (bottom right) Output eye patterns at 10 Gb/s data rate with a PRBS pattern of 2^{31}-1.

Figure 8(a) shows the block diagram of the setup used to measure the eye patterns and BER of the proposed BOSA. The commercial evaluation board (Finisar, SFP + evaluation board and SFP + module) is used to obtain the eye patterns and BER. The modulated optical signals are transmitted from transmitting part of SiOB 1 to a PD of commercial SFP + module via a 100 m long MMF. The generated photocurrent from the PD inside of SFP + module is amplified by the TIA of SFP + module. The amplified electrical data signal is divided using a T RF adapter connector 3 way splitter. The divided electrical data signal is then fed to a wide-bandwidth oscilloscope and an error detector. Figure 8(b) shows the measured eye patterns in accordance with a 5 Gb/s and 10 Gb/s data rate with a PRBS pattern of 2^{31}-1. In case of a bias current of 6 mA, the measured peak-to-peak jitter for 5 Gb/s and 10 Gb/s are

31.92 ps and 37.38 ps, respectively. However, when the bias current was increased to 9 mA, the peak-to-peak jitter for 5 Gb/s and 10 Gb/s eye patterns was decreased to 20.77 ps and 22.02 ps, respectively. The BER was measured using error detector, and it was observed to less than 10^{-12}. From the measurements and clear eye patterns, it can be concluded that the proposed BOSA can be safely operated at a data rate of the 10 Gb/s without any error.
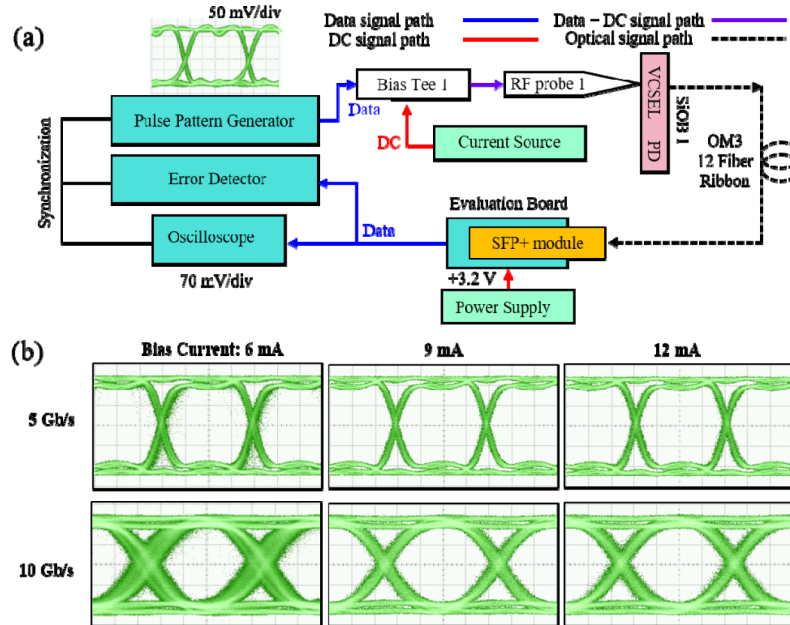

Fig. 8. (a) Experimental setup for measuring BER and eye patterns with TIA. (b) Measured eye patterns at a data rate of 5 Gb/s and 10 Gb/s using a PRBS pattern of 2^{31}-1 for various bias currents of VCSEL.

5. Conclusion

In this paper, a SiOB-based BOSA having high optical alignment accraucy and high coupling efficiency is demonstrated in which the fibers are inserted and held using TFGHs. DRIE process is used to fabricate the TFGH. CPW Tline used for carrying the RF signal was fabricated on high-resistivity substrate and showed a low insertion loss of −0.52 dB at 10 GHz. The 4 channel Tx part of the proposed BOSA using passive optical alignment method shows outstanding coupling efficiency without adding any coupling optics. The clearly open eye patterns and a very low BER of 10^{-12} at 10 Gb/s data rate of the proposed BOSA verify that the BOSA is suitable as a 4 channel × 10 Gb/s optical interconnect module. The proposed BOSA can be realized with low cost since all the components can be packaged by passive alignment techniques and can attain good coupling efficiency.

7. Acknowledgment